PHYSICAL REVIEW B **84**, 104403 (2011)

Nonlinear and spin-glass susceptibilities of three site-diluted systems

Julio F. Fernández
Instituto de Ciencia de Materiales de Aragón, CSIC-Universidad de Zaragoza, ES-50009-Zaragoza, Spain and Instituto Carlos I de Física Teórica y Computacional, Universidad de Granada, ES-18071 Granada, Spain
(Received 4 July 2011; revised manuscript received 11 August 2011; published 1 September 2011)

The nonlinear magnetic χ_3 and spin-glass χ_{SG} susceptibilities in zero applied field are obtained from tempered Monte Carlo simulations for three different spin glasses (SGs) of Ising spins with quenched site disorder. We find that the relation $-T^3\chi_3 = \chi_{SG} - 2/3$ (T is the temperature), which holds for Edwards-Anderson SGs, is approximately fulfilled in canonical-like SGs. For nearest-neighbor antiferromagnetic interactions on a 0.4 fraction of all sites in face-centered cubic (fcc) lattices, as well as for spatially disordered Ising dipolar (DID) systems, $-T^3\chi_3$ and χ_{SG} appear to diverge in the same manner at the critical temperature T_{SG}. However, $-T^3\chi_3$ is smaller than χ_{SG} by over two orders of magnitude in the diluted fcc system. In DID systems, $-T^3\chi_3/\chi_{SG}$ is very sensitive to the system's aspect ratio. Whereas, near T_{SG}, χ_{SG} varies by approximately a factor of 2 as system shape varies from cubic to long-thin-needle shapes, χ_3 sweeps over some four decades.

DOI: 10.1103/PhysRevB.84.104403 PACS number(s): 75.10.Nr, 75.50.Lk, 75.30.Kz, 75.40.Mg

I. INTRODUCTION

The existence of an equilibrium phase transition into the spin glass (SG) phase has not yet been convincingly established for some spin glasses. The development of the *parallel tempered* Monte Carlo (TMC) algorithm[1] has enabled one to observe, bypassing anomalously long relaxation processes, SG models in *equilibrium* at low temperatures. Thus, correlation lengths ξ have been determined from the equilibrium behavior of $\langle\langle s_i s_j\rangle_T^2\rangle_q$, where $s_i = \pm 1$ is for a spin at site i, and $\langle\ldots\rangle_T$ and $\langle\ldots\rangle_q$ stand for a thermal average and for an average over quenched randomness, respectively. There is evidence, from Monte Carlo simulations, that ξ grows as linear system size L in (i) the Edwards-Anderson (EA) model[2,3] at some nonzero temperature T_{SG} in three dimensions, in (ii) geometrically frustrated systems, such as strongly site-diluted Ising models, with nearest-neighbor antiferromagnetic (AF) bonds, on face-centered cubic (fcc) lattices,[4,5] and in (iii) strongly site-diluted Ising models with dipole-dipole interactions, such as in $LiHo_xY_{1-x}F_4$.[6] We refer to the latter systems as disordered Ising dipolar (DID) systems.[7,8] At least for DID systems, some numerical evidence that is unfavorable for the existence of a phase transition also exists.[9] The divergence of ξ implies the divergence of the so-called spin-glass susceptibility χ_{SG} at T_{SG}, where $\chi_{SG} = N^{-1}\sum_{ij}\langle\langle s_i s_j\rangle_T^2\rangle_q$ and N is the number of spins.

Convincing experimental evidence for the existence of an equilibrium phase transition into the SG phase is harder to obtain. This is mainly because (i) very long relaxation processes make equilibrium observations difficult, and (ii) neither ξ nor χ_{SG} can be directly observed. Instead, the SG transition is usually characterized by the nonlinear magnetic susceptibility χ_3.[10] It is defined by

$$m = \chi_1 H + \chi_3 H^3 + \ldots, \tag{1}$$

assuming $m(-H) = -m(H)$. Canella and Mydosh[11] were first able to measure (in gold-iron alloys) huge values of χ_3: $T_{SG}^2\chi_3/\chi_1 \sim 10^5$ (from here on, we let Boltzmann's constant and Bohr's magneton equal 1) near $T = T_{SG}$. Later, χ_3 was shown[12] to diverge in other canonical SGs as a power of $T - T_{SG}$. For the EA model,[13] originally inspired by the discovery of Canella and Mydosh, Chalupa[14] showed long ago that

$$-\chi_3 = T^{-3}(\chi_{SG} - 2/3) \tag{2}$$

if no field is applied. Thus, the critical behavior of χ_3 and χ_{SG}, which one observes in simulations, can, at least for the EA model, be clearly related to the critical behavior of χ_3, which one observes experimentally.

The three models we study are governed by the Hamiltonian

$$\mathcal{H} = -\frac{1}{2}\sum_{ij} J_{ij} x_i s_i x_j s_j, \tag{3}$$

where the sum is over all i and j lattice sites, J_{ij} is model specific, $x_i = \pm 1$ is a quenched random variable, and s_i is a (± 1) Ising spin at site i. All sites are occupied with the same probability $x = \langle x_i\rangle_q$, where the q subscript stands for a quenched average over all site occupancy arrangements.

The aim of this paper is to find how $-\chi_3$, an experimentally measured quantity, and χ_{SG}, a quantity that is often calculated, are related in site-diluted SGs. More specifically, numerical results from TMC are sought for (i) Ising spins, with Ruderman-Kittel-Kasuya-Yoshida (RKKY) interactions,[15] which are randomly located on a small fraction of all lattice sites, (ii) a geometrically frustrated Ising spin system, mainly, randomly located Ising spins, with nearest-neighbor AF interactions, on a 0.4 fraction of all sites of an fcc lattice, and (iii) DID systems on a small fraction of all lattice sites. The outcome of these calculations is unknown because Eq. (2) has not been derived for site-diluted SGs. On the other hand, χ_3 and χ_{SG} can exhibit the same critical behavior in site-diluted SGs if they and the EA model belong to the same universality class. This has been predicted[16] to be so for the first of the above three models, but not so, as far as we know, for the other two models.[17,18]

An outline of the paper follows. Details about the procedure we follow in our calculations are given in Sec. II. For various sizes of each of these systems, we obtain ξ/L, χ_{SG}, and χ_3. Data for ξ/L are used to establish the phase transition temperature T_{SG} between the paramagnetic and SG phases. We then compare how χ_{SG} and χ_3 vary with system size and with temperature in the vicinity of T_{SG}. The results obtained for

TABLE I. Values for T_{SG} follow from crossing (or merging) points of ξ/L curves for various values of system linear size L. Values of η are assigned so that $\chi_{SG}/L^{2-\eta}$ curves for various L values cross at T_{SG}. Errors in η follow from errors in T_{SG}. As explained in Ref. 8, T_{SG} can be obtained for DID systems [for all $x \lesssim 0.5$ in sc lattices (Ref. 8) and $x \lesssim 0.25$ in (Ref. 24) $LiHo_xY_{1-x}F_4$] from the T_{SG} value given below, making use of $T_{SG} \propto x$. Similarly, for RKKY interactions and all $x \lesssim 0.1$.

	RKKY	fcc	DIDs
T_{sg}	0.10(4) for $x = 0.1$	0.4(1) for $x = 0.4$	0.35(4) for $x = 0.35$
η	−0.5(4)	−0.5(2)	0.0(3)

each system are given in each of the sections of Sec. III. Very briefly, these results follow. We find that χ_3 approximately follows Eq. (1) in strongly diluted systems of Ising spins with RKKY interactions. On the other hand, $-T^3\chi_3$ is a over a couple of orders of magnitude smaller than χ_{SG} in a ($x = 0.4$) site-diluted AF Ising model on an fcc lattice. Nevertheless, both χ_3 and χ_{SG} appear to have the same critical behavior. Finally, in DID systems, $-T^3\chi_3$ and χ_{SG} seem to diverge similarly at T_{SG}. However, $-T^3\chi_3/\chi_{SG}$ varies sharply with the systems' shape. Taking into account demagnetization effects, we estimate in Sec. IV how $-T^3\chi_3$ varies with system shape for high aspect ratios. Near the transition temperature, $-T^3\chi_3/\chi_{SG}$ increases from $-T^3\chi_3/\chi_{SG} \sim 10^{-2}$ for cubic shape systems to $-T^3\chi_3/\chi_{SG} \sim 10^2$ for very thin long prisms. Our conclusions are summarized in Sec. V.

As a by-product, we have obtained values for η and T_{SG} in these three systems. They are listed in Table I. From here on, in addition to $k_B = 1$, $\mu_B = 1$, we let $m = N^{-1}\sum_i \langle\langle s_i\rangle_T\rangle_q$, and assume spins in all models point up or down along the z axis, sometimes referred to as the magnetization axis.

II. PROCEDURE

To calculate χ_3, we make use of

$$6\chi_3 = N^{-1}T^{-3}\big(\langle M^4\rangle_T - 3\langle M^2\rangle_T^2\big), \quad (4)$$

where $M = Nm$, which holds for $H = 0$. This equation follows from Eq. (1) by (i) repeated differentiation with respect to H of the canonical ensemble average expression for $\langle m\rangle_T$, and by (ii) letting $\Delta = 0$, where $\Delta = -4\langle M^3\rangle\langle M\rangle + 12\langle M^2\rangle\langle M\rangle^2 - 6\langle M\rangle^4$. This is justified for finite systems with up-down symmetry if averages are taken over infinite times since $\langle M^n\rangle = 0$ then for all odd n. The order in which system sizes and averaging times are taken to infinity is irrelevant for the paramagnetic phase. Equations (2) and (4), as well as all the results below, are only claimed to hold for $T \geqslant T_{SG}$. Note that Eq. (4) is valid for each realization of quenched disorder. Chalupa derived Eq. (2) from Eq. (4) for the EA model by first averaging over all system samples and noting that (i) both $\langle M^4\rangle$ and $\langle M^2\rangle^2$ involve sums over four-spin terms, such as $\sum_{ijkl}\langle\langle s_is_js_ks_l\rangle_T\rangle_q$ and $\sum_{ijkl}\langle\langle s_is_j\rangle_T\langle s_ks_l\rangle_T\rangle_q$, respectively, and (ii) any term in which one or more subindices is unpaired vanishes. To see this, assume the k index is unpaired in either of the two sums over $ijkl$ indices. Now, consider all exchange bonds J_{km} between the kth and any other site. Let us assume the probabilities for J_{km} and $-J_{km}$ for all m, while all other exchange constants remain unchanged, are equal. (This requires exchange bonds to be *independently* random.) It follows that the probabilities for s_k and $-s_k$, for any given configuration of all the other spins, are equal. This is the gist of the proof. For further details, see Ref. 14. The proof fails for site-diluted systems because exchange bonds are not then *independently* random.

We simulate a set of identical systems at temperatures T_{min}, $T_{min} + \Delta T$, $T_{min} + 2\Delta T, \ldots, T_{max}$ following standard TMC rules.[1] We choose $T_{max} \simeq 2.5T_{SG}$, $T_{min} \sim 0.5T_{SG}$, and all ΔT such that at least 30% of all attempted exchanges between systems at T and $T + \Delta T$ are successful for all T. We let each system equilibrate for a time τ_s and take averages over an equally long subsequent time τ_s. Time τ_s satisfies two requirements: (i) $\langle\langle M\rangle_T^2\rangle_q \ll 0.1\langle\langle M^2\rangle_T\rangle_q$ obtains for all $T \in [T_{min}, T_{max}]$, and (ii) systems that start from either random configurations or from (assumed) equilibrium configurations come to the same condition, as specified in Ref. 19, after time τ_s. Values of τ_s, of the number of samples N_s with different quenched randomness over which averages were taken, and of the site occupancy rate x, are given in Table II. Periodic boundary conditions are used throughout. For DID systems, we make use of Ewald sums.[20]

For the correlation length ξ, we make use, as has become standard practice,[2,8,19,21] of the original definition[22]

$$\xi^2 = \frac{1}{4\sin^2(k/2)}\left[\frac{\chi_{SG}}{|\ \chi_{SG}(\mathbf{k})\ |} - 1\right], \quad (5)$$

where $\chi_{SG}(\mathbf{k}) = N^{-1}\sum_{ij}\langle\langle s_is_j\rangle_T^2\rangle_q \exp(i\mathbf{k}\cdot\mathbf{r}_{ij})$, and we let $\mathbf{k} = (2\pi/L,0,0)$. Note that $\chi_{SG}(\mathbf{k} = 0) = \chi_{SG}$ and that, as $L \to \infty$, ξ/L vanishes in the paramagnetic phase, remains finite at $T = T_{SG}$, and either grows without bounds below T_{SG}, as in a conventional phase transition, or remains finite as in the XY model in two dimensions. The point where ξ/L curves for various system sizes meet as T decreases defines T_{SG} for us.

All systems we report on below have a common feature: fractional errors for χ_3 are an order of magnitude larger than those for χ_{SG} and for χ_1. Unless otherwise stated, error bars

TABLE II. The number of samples N_s and the number of Monte Carlo sweeps τ_s that were taken both for equilibration and for the subsequent averaging times are given in thousands of Monte Carlo sweeps. There are L^3 lattice sites in RKKY and fcc systems, but $L \times L \times 2L$ lattice sites for DID systems.

	RKKY			fcc				DID		
L	6	8	12	4	6	8	12	4	6	8
τ_s	10	40	400	10	10	40	40	10	100	3000
N_s	100	40	10	10	40	10	5.6	100	15	4
x	0.1	0.1	0.1	0.4	0.4	0.4	0.4	0.35	0.35	0.35

are given for χ_3 and related quantities, but not for χ_{SG} or χ_1, which are all smaller than icons for their data points.

III. RESULTS

All results in this section follow from TMC simulations.

A. Spatially disordered Ising spins with RKKY interactions

The Hamiltonian is given by Eq. (3), with $J_{ij} = \varepsilon_c(\cos kr_{ij})(a/r_{ij})^3$, i.e., an RKKY (Ref. 15) interaction, as in a canonical spin glass. We let $ka = 2\pi$, where a is a nearest-neighbor distance, and ε_c is an energy in terms of which all temperatures are given in this section. We let each site is be occupied with $x = 0.1$ probability.

Plots of ξ/L versus T for various system sizes are shown in Fig. 1(a). Not all pairs of curves cross at the same point. Let $T_{i,j}$ be the temperature where curves for lengths L_i and L_j cross, where $L_1 = 6$, $L_2 = 8$, and $L_3 = 12$. Plots of T_{ij} (where $T_{1,2} = 0.29$, $T_{1,3} = 0.23$, and $T_{2,3} = 0.20$) versus $1/L_iL_j$ fall onto a straight line, which extrapolates to $T = 0.10$ as $1/L_iL_j \to 0$. We, thus, estimate $T_{SG} = 0.10$ and therefore expect $T/x = 1.0$ for $x \lesssim 1$ values since the $1/r^3$ dependence of the interaction implies[8] $\xi(x,T) = \xi(T/x)$.

In Fig. 1(b), we can see that χ_{SG} seems to grow without bounds with system size at $T = T_{SG}$. Indeed, we note that $\chi_{SG} \sim L^{2-\eta}$, where $\eta \simeq -0.5$ at T_{SG}. This η value at the boundary of the range $-0.5 \lesssim \eta \lesssim -0.2$ of quoted[3] values, from Monte Carlo simulations, for the EA model. We note in passing that this model and the EA model have been predicted[16] to be in the same universality class.

How $-T^3\chi_3$ behaves near T_{SG} is shown in Fig. 2(a). It varies with T and with L much as χ_{SG} does in Fig. 1(b). The plots shown in Fig. 2(b) are consistent with $-T^3\chi_3 \sim \chi_{SG}$. [The value $\eta = -0.5$ follows from the plots shown in Fig. 1(b), not from any fitting of χ_3 to any desired behavior.] More significantly, $-T^3\chi_3/\chi_{SG}$ appears to approach a *smooth* function of temperature in the neighborhood of $T = T_{SG}$ as $L \to \infty$. This is the basis for the main conclusion of this section, namely, that $-T^3\chi_3$ and χ_{SG} have the same critical behavior.

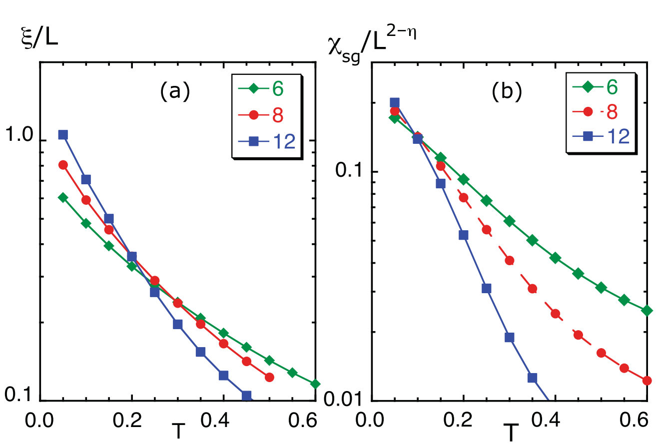

FIG. 1. (Color online) (a) Semilog plots of ξ/L vs T for (±1) Ising spins with RKKY interactions, randomly located, on a 0.1 fraction of all L^3 sites. The numbers in the box are L values. (b) Same as in (a) but for $\chi_{SG}/L^{2-\eta}$ vs T, for $\eta = -0.5$.

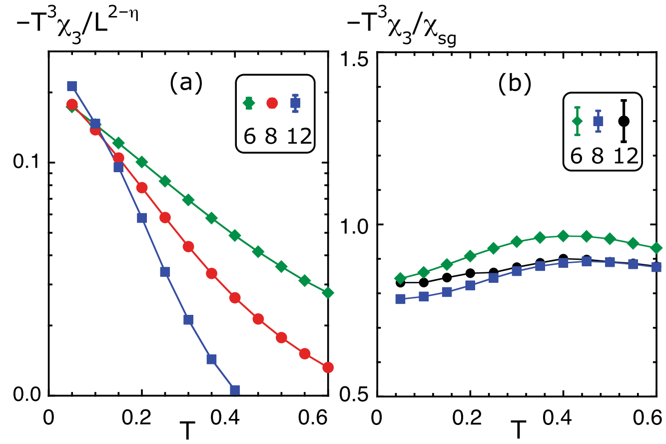

FIG. 2. (Color online) (a) Semilog plots of $-T^3\chi_3/L^{2-\eta}$ vs T, for $\eta = -0.5$, for (±1) Ising spins with RKKY interactions, randomly located, on a 0.1 fraction of L^3 sites, for the values of L, which are shown in the box. (b) Same as in (a) but for $-T^3\chi_3/\chi_{SG}$ vs T.

B. Site-diluted AF Ising model on a fcc lattice

Each site of a fcc lattice is occupied with a (±1) Ising spin with a 0.4 probability. The Hamiltonian is given by Eq. (3), with $J_{ij} = -J$ if i and j are nearest neighbors but $J_{ij} = 0$ otherwise. A 0.4 occupancy rate is roughly midway between the lowest value $x = 0.195$ for percolation[23] in fcc lattices and the transition point $x \simeq 0.75$ between SG and AF phases.[4] All temperatures are given in terms of J.

Monte Carlo results for this model are shown in Figs. 3(a) and 3(b). We note in Fig. 3(a) that the crossing point between pairs of ξ/L curves drifts leftward as their L values increase. As for Fig. 1(a), let $T_{i,j}$ be the temperature where curves for lengths L_i and L_j cross, where $L_1 = 4$, $L_2 = 6$, $L_3 = 8$, and $L_4 = 12$. A second-degree polynomial fit to a plot of T_{ij} (where $T_{1,2} = 0.70$, $T_{1,3} = 0.67$, $T_{1,4} = 0.62$, $T_{2,3} = 0.62$, $T_{2,4} = 0.57$, and $T_{3,4} = 0.53$) versus $1/L_iL_j$ gives $T_{ij} \to 0.4$ as $1/L_iL_j \to 0$. We thus estimate $T_{SG} = 0.4(1)$, in agreement, within errors, with the values found for $x = 0.4$ in Ref. 4. Plots of $\chi_{SG}/L^{2-\eta}$ versus T are shown in Fig. 3(b) for $\eta = -0.5$.

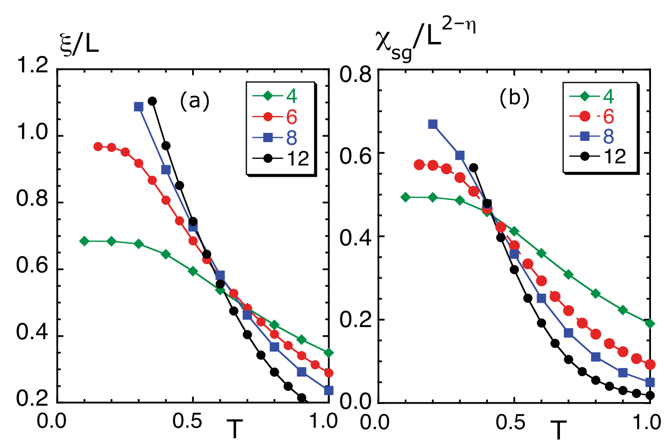

FIG. 3. (Color online) (a) Plots of ξ/L vs T for a ($x = 0.4$) site-diluted AF Ising model on an fcc lattice of $L \times L \times L$ sites. The numbers in the box are L values. (b) Same as in (a) but for $\chi_{SG}/L^{2-\eta}$ vs T, for $\eta = -0.5$.

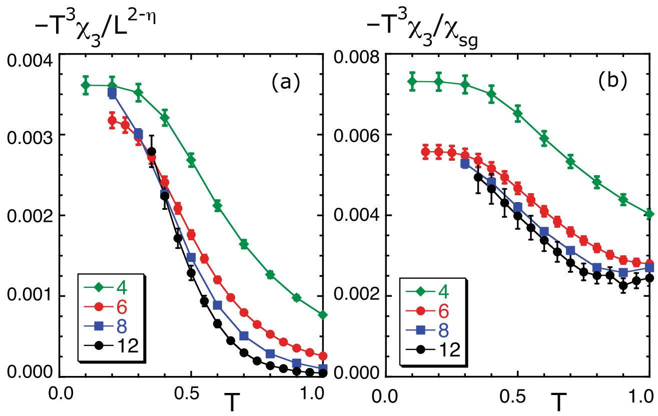

FIG. 4. (Color online) (a) Plots of $-T^3\chi_3/L^{2-\eta}$ vs T, for $\eta = -0.5$, for a ($x = 0.4$) site-diluted AF Ising model on an fcc lattice of $L \times L \times L$ sites. The numbers in the box are L values. (b) Same as in (a) but for $-T^3\chi_3/\chi_{SG}$ vs T.

This is the best value of η to have $\chi_{SG}/L^{2-\eta}$ curves for various values of L cross at T_{SG}. This value of η is, within errors, in agreement with the value found for $x = 0.4$ in Ref. 4.

Plots of $-T^3\chi_3/L^{2-\eta}$ versus T, with $\eta = -0.5$, are shown in Fig. 4(a). The $\eta = -0.5$ value is taken from the plots of $\chi_{SG}/L^{2-\eta}$ versus T, not from any fitting of χ_3 to any desired behavior. The curves in Figs. 3(b) and 4(a) are somewhat different, but all curves for $L = 6$, 8, and 12 in both figures do cross, *within errors*, at the same temperature $T_{SG} = 0.4$.

In Fig. 4(b), we notice that $-T\chi_3 \ll \chi_{SG}$, which differs markedly from what might have been expected from the behavior of the EA model (and from the above results for SGs with RKKY interactions). More significantly, we observe $-T\chi_3/\chi_{SG}$ is, within errors, independent of L for the largest values of L, and appears to go into a smooth function of T, near T_{SG}, as $L \to \infty$. This suggests that, in the thermodynamic limit, both quantities have the same critical behavior.

C. Spatially disordered (±1) Ising dipoles

Here, we consider disordered Ising dipolar (DID) systems in simple cubic (SC) lattices. We let each site be occupied, with a 0.35 probability, by a (±1) spin. All spins point up and down, along the z axis. The Hamiltonian is given by Eq. (3), with

$$J_{ij} = h_d \left(\frac{a}{r_{ij}^3}\right)^3 \left(3\frac{z_{ij}^2}{r_{ij}^2} - 1\right), \qquad (6)$$

where r_{ij} is the distance between i and j sites, z_{ij} is the z component of r_{ij}, h_d is an energy, and a is the SC lattice constant.

Let us first recall that, despite some earlier numerical evidence to the contrary,[9] more recent calculations point to the existence of a phase transition between the paramagnetic and SG phases in diluted Ising dipolar systems[7,8] at $T_{SG}/x \simeq 1$ for all $x \lesssim 0.5$. In addition,[19] $\chi_{SG} \sim L^{2-\eta}$ at $T = T_{SG}$, where $\eta \simeq 0$.

We deal with the *magnetic* susceptibility here which, as is well known, depends on the shape of the system.[25] For this reason, we study numerically $L \times L \times nL$ shaped prism systems for various values of n, that is, square-base prisms with a 1 : n aspect ratio.

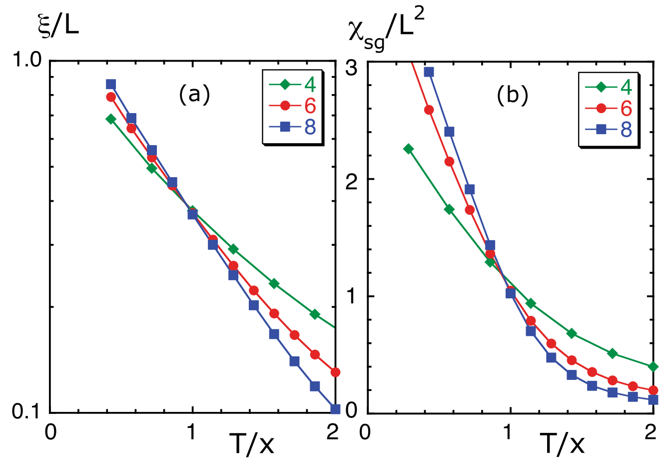

FIG. 5. (Color online) (a) Semilog plots of ξ/L vs T/x for DID systems on a 0.35 fraction of all $L \times L \times L_z$ sites, where $L_z = 2L$. The numbers in the box are L values. (b) Same as in (a) but for χ_{SG}/L^2 vs T/x. Error bars are smaller than icons for all data points.

Plots of ξ/L versus T/x are shown in Fig. 5(a) for $n = 2$. Curves for three different values of L are observed to cross at $T/x \simeq 1.0$. This transition temperature value is in agreement with the result found in Ref. 8 for $n = 1$, mainly, that $T_{SG}/x \simeq 1.0$ for all $x \lesssim 0.5$. Plots of χ_{SG}/L^2 versus T/x are shown in Fig. 5(b). All curves are observed to cross at $T/x = 0.95$. This is approximately as in Ref. 8.

We now turn our attention to the *magnetic* susceptibility. Plots of $-T^3\chi_3/L^2$ versus T/x are shown in Fig. 6(a) for systems of various sizes. These plots resemble those for χ_{SG} in Fig. 5(b), but note that the crossing points are not quite at the same temperature in the two figures.

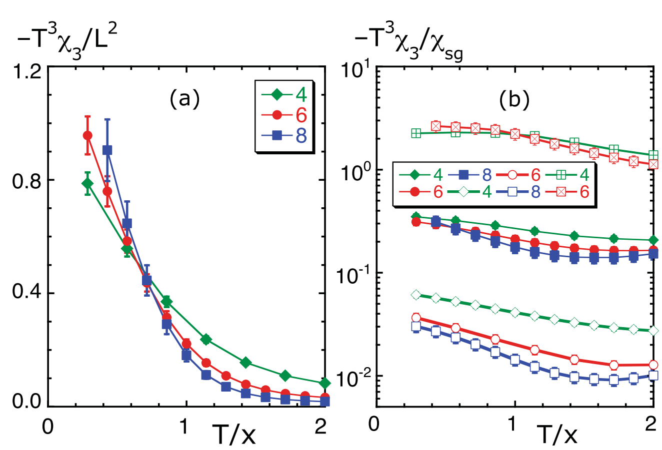

FIG. 6. (Color online) (a) Plots of $-T^3\chi_3/L^2$ vs T/x for DID systems on a 0.35 fraction of all $L \times L \times L_z$ sites, where $L_z = 2L$. (b) Plots of $-T^3\chi_3/\chi_{SG}$ vs T/x for three 1 : n aspect ratios, $n = 4$ (⊞ and ⊠) for the two top curves, $n = 2$ (full icons) for the three curves in the middle, and $n = 1$ (empty icons) for the three lower curves. Error bars hardly protrude from icons. For both (a) and (b), the numbers in the box are the values of L.

In order to better compare $-T^3\chi_3$ and χ_{SG}, we plot in Fig. 6(b) the ratio $-T^3\chi_3/\chi_{SG}$ versus T/x for systems of various sizes with 1 : 4, 1 : 2, and 1 : 1 aspect ratios. For a 1 : 4 aspect ratio, only data points for systems with $4 \times 4 \times 16$ and $6 \times 6 \times 24$ sites appear in Fig. 6(b). A larger system with the same aspect ratio would have taken a prohibitively long computer time to run. Let $L_\star$ be a system length such that $-T^3\chi_3/\chi_{SG}$ is approximately size independent if $L \gtrsim L_\star$. Clearly, $L_\star \simeq 4$ and 6 for $n = 4$ and 2, respectively, in Fig. 6(b). For $n = 1$, $L_\star \simeq 8$ seems likely. This would be in accordance with the expectation that $-T^3\chi_3$ and χ_{SG} have the same critical behavior in DID systems, independently of aspect ratio.

Questions about the sharp variation of $-T^3\chi_3/\chi_{SG}$ with respect to aspect ratio naturally arise. What is the asymptotic behavior of $-T^3\chi_3/\chi_{SG}$? This is hard to foresee from the data plots shown in Fig. 6(b). To proceed much further numerically is impractical. The next section is devoted to this question.

IV. VARIATION OF χ_3 WITH ASPECT RATIO IN DID SYSTEMS

In this section, we derive an approximate equation for the variation of χ_3 with shape in DID systems. Consider two systems of the same shape and size. In system f, all spin pairs interact. In the other system, system t, dipole-dipole interactions are truncated. In t, each spin interacts only with spins that lie within a long thin cylinder centered on it, the axis of which is parallel to the system's z axis. The radius of the cylinder need not be more than a couple of nearest-neighbor distances, but its length must be much longer than its radius. Let us furthermore assume that both systems are homogeneous, that is, all sites are occupied ($x = 1$). Now, we know from Ref. 26 that if both systems are in thermal equilibrium, and external magnetic fields H_t and H_f are applied to systems t and f, respectively, such that m is the same in both systems, then

$$H_f = H_t - \lambda_n m, \tag{7}$$

where n comes from f system's 1 : n aspect ratio. Equation (7) holds because the only effect of the *un*truncated portion of all dipole-dipole interactions in f is to give the so-called *demagnetizing* field $-\lambda_n m$. For *dipolar* prisms of 1 : n aspect ratio, a scaling expression such as[27] $m = t^{-\beta} f(Ht^{-\beta\delta})$ must therefore be replaced by

$$m = t^{-\beta} f[(H - \lambda_n m)t^{-\beta\delta}], \tag{8}$$

where H_f has been replaced by H.

Taking the derivative of Eq. (8) with respect to H [or, more simply, of Eq. (7) with respect to m] gives

$$\frac{1}{\chi_1(n)} = \frac{1}{\chi_1(\infty)} + \lambda_n, \tag{9}$$

where $\chi_1(n)$ is the linear susceptibility of a prism with a 1 : n aspect ratio, and, clearly, $dm/dH_t = \chi_1(\infty)$. This is the well-known equation[25] that experimentalists[6,28] often use in order to do away with demagnetization effects, and thus relate $\chi_1(n)$, the measured susceptibility, to $\chi_1(\infty)$.

Taking the d/dH_t derivative of Eq. (9) gives

$$\left(1 + \lambda_n \frac{dm}{dH_t}\right) \frac{1}{\chi_1^2(n)} \frac{d\chi_1(n)}{dH_n} = \frac{1}{\chi_1^2(\infty)} \frac{d\chi_1(\infty)}{dH_t}, \tag{10}$$

where we have used $dH_n/dH_t = 1 + \lambda_n dm/dH_t$, which follows from Eq. (7). We next (i) take the d/dH_t derivative of the above equation, (ii) let $H_t = H_n = 0$, and (iii) let $d\chi_1(\infty)/dH_t = 0 = d\chi_1(n)/dH_n$ by up-down symmetry. The result is easily cast into

$$\chi_3(n) = \frac{\chi_3(\infty)}{[1 + \lambda_n \chi_1(\infty)]^4}, \tag{11}$$

which is the desired expression relating $\chi_3(n)$ and $\chi_3(\infty)$.

Equations (9) and (11) enable us to calculate how $\chi_3(n)$ varies with n if we know χ_1 and χ_3 for at least an aspect ratio each, as well as λ_n. A list of (easily computed) λ_n values for several values of $n \in [0.5,7]$, as well as a functional relation for all $n \geqslant 8$, are given in Table III. Since the only effect of the long-range portion of all dipole-dipole interactions in f is to give the demagnetizing field[26] $-\lambda_n m$, we can calculate all λ_n assuming a fully occupied lattice in which all spins point up. Since only a single state comes into the calculation, no Monte Carlo simulation is necessary. This enables us to calculate λ_n for very large systems. The fact that only an x fraction of lattice sites is occupied in site-diluted SGs is *approximately* taken into account by letting $\lambda_n \to x\lambda_n$ everywhere. Inhomogeneities in SGs are thus neglected.

Equation (9) gives the three dashed lines shown in Fig. 7(a) for $\chi_1(\infty) = 7, 9$, and 11. With two of these values, we obtain from Eq. (11) the three curves for $\chi_3(n)$ shown in Fig. 7(b) for values of $\chi_3(\infty)$. These curves do not fit the data points too well. On the other hand, a good fit for small system sizes should not be expected. We can nevertheless conclude with some confidence that $\chi_3(n)$ does not diverge as $n \to \infty$. Indeed, $\chi_3(\infty)$ is most likely within the (50,120) range. Furthermore, observation of Fig. 7(b) indicates that $\chi_3(n)/\chi_{SG}$ at $T = T_{SG}$ varies over three or four orders of magnitude as system shape varies from cubic to infinitely thin needlelike.

It is perhaps worth pointing out that

$$\chi_3(n) = \frac{\chi_3(\infty)}{\chi_1^4(\infty)} \chi_1^4(n) \tag{12}$$

follows immediately from Eqs. (9) and (11) after Eq. (9) is cast into $\chi_1(n) = \chi_1(\infty)/[1 + \lambda_n \chi_1(\infty)]$. Equation (12) implies that χ_3 sweeps over four times as many decades as χ_1 does [compare Figs. 7(a) and 7(b)] as n varies.

Finally, note that the classical or quantum nature of DID systems does not play any role in this section. It does not matter

TABLE III. λ_n values, in terms of h_d, for some n in the [0.5,7] range. For $n \geqslant 8$, $\lambda_n \simeq 8/n^2$. For an x site occupancy rate, $\lambda_n \to x\lambda_n$.

n	0.5	1	1.5	2	2.5	3	4	5	6	7
λ_n	7.419	4.189	2.503	1.611	1.107	0.802	0.471	0.308	0.217	0.160

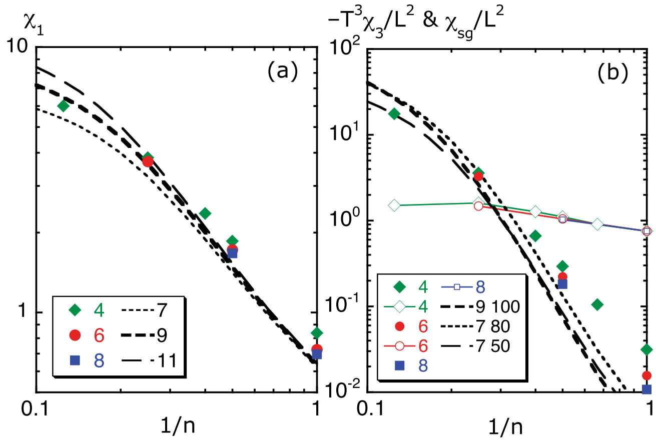

FIG. 7. (Color online) (a) Plots of χ_1 vs $1/n$ for DID systems at $T = T_{\rm SG}$ on a 0.35 fraction of all $L \times L \times nL$ sites. The shown numbers are L values for data points from Monte Carlo calculations. The dashed lines follow from Eq. (9), assuming the three values for $\chi_1(\infty)$ that are shown in the box. (b) Same as in (a) but for (full icons) $-T^3\chi_3/L^2$ and (open icons) $\chi_{\rm SG}/L^2$. The dashed lines follow from Eqs. (9) and (11), and the shown pairs of values, such as 9 and 100, are for $\chi_1(\infty)$ and $\chi_3(\infty)$, respectively.

either whether a transverse field is applied because it does not affect up-down symmetry. These equations can therefore be applied, as an illustration, to $\mathrm{Li}_1 - x\mathrm{Ho}_x\mathrm{Y}_4$, under a transverse field, as in Ref. 24, where $T^2\chi_3/\chi_1 \sim 1$ was observed on a $1.6 \times 16 \times 5$ mm^3 sample. Values of χ_1 and χ_3 that would be some 3 and 100 times larger, respectively, for a long-thin-needlelike sample can be read off from Figs. 7(a) and 7(b).

V. CONCLUSIONS

By the tempered Monte Carlo method,[1] we have tested whether the relation $-T^3\chi_3 = \chi_{\rm SG} - 2/3$, which is known[14] to hold for the Edwards-Anderson model, also holds for several site-diluted spin glasses of (± 1) Ising spins, with (i) RKKY interactions, (ii) antiferromagnetic interactions between nearest-neighbor spins on fcc lattices, and (iii) dipole-dipole interactions. As a by-product, we have obtained the values of η and T_{sg} that are listed in Table I.

We have found $-T^3\chi_3 \sim \chi_{\rm SG}$ to hold for Ising spins with RKKY interactions occupying a 0.1 fraction of all lattice sites. More significantly, $-T^3\chi_3/\chi_{\rm SG}$ appears to be (i) independent of linear system size, within errors, and (ii) a smooth function of temperature near $T_{\rm SG}$. This suggests $-T^3\chi_3$ and $\chi_{\rm SG}$ have the same critical behavior. Since the RKKY interaction decays as the inverse of the cube of the distance, these results must hold for lower values of x if the temperature is scaled with x.

We have found $-T^3\chi_3$ to be over two orders of magnitude smaller than $\chi_{\rm SG}$ for Ising spins, with antiferromagnetic interactions, on a ($x = 0.4$) site-diluted fcc lattice. Our results are, however, consistent with identical critical behavior of these two quantities.

In DID systems, the TMC data [see Fig. 6(b)] are consistent with χ_3 and $\chi_{\rm SG}$ diverging in the same manner as $T \to T_{\rm SG}$ from above. The sharp variation of $-T^3\chi_3/\chi_{\rm SG}$ with aspect ratio, which can be observed in Fig. 6(b), is noteworthy. How this comes about from demagnetization effects is explained in Sec. IV. In it, relations are derived, which together with data points coming from TMC simulations [see Fig. 7(b)] give rough estimates of $-T^3\chi_3$ at or near $T = T_{\rm SG}$. We find $-T^3\chi_3/\chi_{\rm SG}$ varies, as shown in Fig. 7(b), from $-T^3\chi_3/\chi_{\rm SG} \sim 10^{-2}$ for cubic shapes to $-T^3\chi_3/\chi_{\rm SG} \sim 10^2$ for long thin needles.

Our results for DID systems with an $x = 0.35$ site occupancy rate can be generalized to smaller values of x. As discussed in Ref. 8, any physical quantity f satisfies $f(x,T) = f(T/x)$ for x quite smaller than x_c, the critical concentration above which there is magnetic order at low temperature (e.g., $x_c \simeq 0.65$ for SC lattices[8] and $x_c \simeq 0.25$ for $\mathrm{LiHo}_x\mathrm{Y}_{1-x}\mathrm{F}_4$).[24]

ACKNOWLEDGMENTS

I am grateful to J. J. Alonso for helpful remarks after reading the manuscript. Funding Grant No. FIS2009-08451 from the Ministerio de Ciencia e Innovación of Spain is acknowledged.

[1]K. Hukushima and K. Nemoto, J. Phys. Soc. Jpn. **65**, 1604 (1996); for recent improvements and discussion, see E. Bittner, A. Nußbaumer, and W. Janke, Phys. Rev. Lett. **101**, 130603 (2008); J. Machta, Phys. Rev. E **80**, 056706 (2009).

[2]See, for instance, M. Palassini and S. Caracciolo, Phys. Rev. Lett. **82**, 5128 (1999); H. G. Ballesteros, A. Cruz, L. A. Fernández, V. Martín-Mayor, J. Pech, J. J. Ruiz-Lorenzo, A. Tarancón, P. Téllez, C. L. Ullod, and C. Ungil, Phys. Rev. B **62**, 14237 (2000).

[3]H. G. Katzgraber, M. Körner, and A. P. Young, Phys. Rev. B **73**, 224432 (2006).

[4]C. Wengel, C. L. Henley, and A. Zippelius, Phys. Rev. B **53**, 6543 (1996).

[5]A. Andreanov, J. T. Chalker, T. E. Saunders, and D. Sherrington, Phys. Rev. B **81**, 014406 (2010).

[6]C. Ancona-Torres, D. M. Silevitch, G. Aeppli, and T. F. Rosenbaum, Phys. Rev. Lett. **101**, 057201 (2008); P. E. Jönsson, R. Mathieu, W. Wernsdorfer, A. M. Tkachuk, and B. Barbara, *ibid.* **98**, 256403 (2007); E. Burzurí, Ph.D. thesis, Universidad de Zaragoza, 2011.

[7]K. M. Tam and M. J. P. Gingras, Phys. Rev. Lett. **103**, 087202 (2009).

[8]J. J. Alonso and J. F. Fernández, Phys. Rev. B **81**, 064408 (2010).

[9]J. Snider and C. C. Yu, Phys. Rev. B **72**, 214203 (2005); A. Biltmo and P. Henelius, *ibid.* **76**, 054423 (2007); **78**, 054437 (2008).

[10]P. W. Anderson, Phys. Today **41**(3), 10 (1988).

[11]V. Canella and J. A. Mydosh, Phys. Rev. B **6**, 4220 (1972); J. A. Mydosh, *Spin Glasses: An Experimental Introduction* (Taylor and Francis, London, 1993).

[12]H. Bouchiat and P. Monod, J. Magn. Magn. Mater. **54**, 124 (1986); B. Barbara, A. P. Malozemoff, and Y. Imry, Phys. Rev. Lett. **47**, 1852 (1981).

[13]S. F. Edwards and P. W. Anderson, J. Phys. F: Met. Phys. **5**, 965 (1975).

[14] J. Chalupa, Solid State Commun. **22**, 315 (1977).

[15] See, for instance, S. Khmelevskyi, J. Kudrnovský, B. L. Gyorffy, P. Mohn, V. Drchal, and P. Weinberger, Phys. Rev. B **70**, 224432 (2004).

[16] A. J. Bray, M. A. Moore, and A. P. Young, Phys. Rev. Lett. **56**, 2641 (1986).

[17] Because of its AF nature, the diluted AF Ising model on a fcc lattice has been expected, in G. S. Grest and E. F. Gabl, Phys. Rev. Lett. **43**, 1182 (1979), to be "less sensitive" to magnetic fields than the EA model.

[18] For skepticism about universality even among variants of the EA model, see L. W. Bernardi, S. Prakash, and I. A. Campbell, Phys. Rev. Lett. **77**, 2798 (1996); L. W. Bernardi and I. A. Campbell, Phys. Rev. B **56**, 5271 (1997); P. O. Mari and I. A. Campbell, Phys. Rev. E **59**, 2653 (1999).

[19] J. F. Fernández, Phys. Rev. B **82**, 144436 (2010).

[20] P. P. Ewald, Ann. Phys. (NY) **369**, 253S, (1921); W. De Leeuw, J. W. Perram, and E. R. Smith, Annu. Rev. Phys. Chem. **37**, 245 (1986); for a more recent account, see, for instance, Z. Wang and C. Holm, J. Chem. Phys. **115**, 6351 (2001).

[21] T. Jörg, H. G. Katzgraber, and F. Krzkakała, Phys. Rev. Lett. **100**, 197202 (2008).

[22] F. Cooper, B. Freedman, and D. Preston, Nucl. Phys. B **210**, 210 (1982); see also Refs. 2 and 19.

[23] J. W. Essam, in *Phase Transitions and Critical Phenomena*, edited by C. Domb and M. S. Green (Academic, New York, 1973), Vol. II, pp. 197–270.

[24] D. H. Reich, B. Ellman, J. Yang, T. F. Rosenbaum, G. Aeppli, and D. P. Belanger, Phys. Rev. B **42**, 4631 (1990).

[25] Perhaps more easily recognized as $\chi_1(\infty) = \chi_1(n)/[1 - \lambda_n \chi_1(n)]$. See, for instance, A. H. Morrish, *The Physical Principles of Magnetism* (Wiley, New York, 2001), Chap. I.

[26] J. F. Fernández and J. J. Alonso, Phys. Rev. B **62**, 53 (2000).

[27] V. Privman and M. E. Fisher, Phys. Rev. B **30**, 322 (1984); *Finite Size Scaling and Numerical Simulation of Statistical Systems*, edited by V. Privman (World Scientific, Singapore, 1990), p. 1; V. Privman, A. Aharony, and P. C. Hohenberg, *Phase Transitions and Critical Phenomena*, edited by C. Domb and J. L. Lebowitz (Academic, New York, 1991), Vol. 14, p. 1.

[28] J. A. Quilliam, S. Meng, C. G. A. Mugford, and J. B. Kycia, Phys. Rev. Lett. **101**, 187204 (2008).